Study of $Z\gamma$ Events and Limits on Anomalous $ZZ\gamma$ and $Z\gamma\gamma$ Couplings in $p\bar{p}$ Collisions at $\sqrt{s} = 1.96$ TeV

V. M. Abazov,[35] B. Abbott,[72] M. Abolins,[63] B. S. Acharya,[29] M. Adams,[50] T. Adams,[48] M. Agelou,[18] J.-L. Agram,[19] S. H. Ahn,[31] M. Ahsan,[57] G. D. Alexeev,[35] G. Alkhazov,[39] A. Alton,[62] G. Alverson,[61] G. A. Alves,[2] M. Anastasoaie,[34] T. Andeen,[52] S. Anderson,[44] B. Andrieu,[17] Y. Arnoud,[14] A. Askew,[48] B. Åsman,[40] A. C. S. Assis Jesus,[3] O. Atramentov,[55] C. Autermann,[21] C. Avila,[8] F. Badaud,[13] A. Baden,[59] B. Baldin,[49] P. W. Balm,[33] S. Banerjee,[29] E. Barberis,[61] P. Bargassa,[76] P. Baringer,[56] C. Barnes,[42] J. Barreto,[2] J. F. Bartlett,[49] U. Bassler,[17] D. Bauer,[53] A. Bean,[56] S. Beauceron,[17] M. Begel,[68] A. Bellavance,[65] S. B. Beri,[27] G. Bernardi,[17] R. Bernhard,[49,*] I. Bertram,[41] M. Besançon,[18] R. Beuselinck,[42] V. A. Bezzubov,[38] P. C. Bhat,[49] V. Bhatnagar,[27] M. Binder,[25] C. Biscarat,[41] K. M. Black,[60] I. Blackler,[42] G. Blazey,[51] F. Blekman,[33] S. Blessing,[48] D. Bloch,[19] U. Blumenschein,[23] A. Boehnlein,[49] O. Boeriu,[54] T. A. Bolton,[57] F. Borcherding,[49] G. Borissov,[41] K. Bos,[33] T. Bose,[67] A. Brandt,[74] R. Brock,[63] G. Brooijmans,[67] A. Bross,[49] N. J. Buchanan,[48] D. Buchholz,[52] M. Buehler,[50] V. Buescher,[23] S. Burdin,[49] T. H. Burnett,[78] E. Busato,[17] J. M. Butler,[60] J. Bystricky,[18] S. Caron,[33] W. Carvalho,[3] B. C. K. Casey,[73] N. M. Cason,[54] H. Castilla-Valdez,[32] S. Chakrabarti,[29] D. Chakraborty,[51] K. M. Chan,[68] A. Chandra,[29] D. Chapin,[73] F. Charles,[19] E. Cheu,[44] D. K. Cho,[68] S. Choi,[47] B. Choudhary,[28] T. Christiansen,[25] L. Christofek,[56] D. Claes,[65] B. Clément,[19] C. Clément,[40] Y. Coadou,[5] M. Cooke,[76] W. E. Cooper,[49] D. Coppage,[56] M. Corcoran,[76] A. Cothenet,[15] M.-C. Cousinou,[15] B. Cox,[43] S. Crépé-Renaudin,[14] M. Cristetiu,[47] D. Cutts,[73] H. da Motta,[2] B. Davies,[41] G. Davies,[42] G. A. Davis,[52] K. De,[74] P. de Jong,[33] S. J. de Jong,[34] E. De La Cruz-Burelo,[32] C. De Oliveira Martins,[3] S. Dean,[43] J. D. Degenhardt,[62] F. Déliot,[18] M. Demarteau,[49] R. Demina,[68] P. Demine,[18] D. Denisov,[49] S. P. Denisov,[38] S. Desai,[69] H. T. Diehl,[49] M. Diesburg,[49] M. Doidge,[41] H. Dong,[69] S. Doulas,[61] L. V. Dudko,[37] L. Duflot,[16] S. R. Dugad,[29] A. Duperrin,[15] J. Dyer,[63] A. Dyshkant,[51] M. Eads,[51] D. Edmunds,[63] T. Edwards,[43] J. Ellison,[47] J. Elmsheuser,[25] V. D. Elvira,[49] S. Eno,[59] P. Ermolov,[37] O. V. Eroshin,[38] J. Estrada,[49] D. Evans,[42] H. Evans,[67] A. Evdokimov,[36] V. N. Evdokimov,[38] J. Fast,[49] S. N. Fatakia,[60] L. Feligioni,[60] T. Ferbel,[68] F. Fiedler,[25] F. Filthaut,[34] W. Fisher,[66] H. E. Fisk,[49] I. Fleck,[23] M. Fortner,[51] H. Fox,[23] S. Fu,[49] S. Fuess,[49] T. Gadfort,[78] C. F. Galea,[34] E. Gallas,[49] E. Galyaev,[54] C. Garcia,[68] A. Garcia-Bellido,[78] J. Gardner,[56] V. Gavrilov,[36] P. Gay,[13] D. Gelé,[19] R. Gelhaus,[47] K. Genser,[49] C. E. Gerber,[50] Y. Gershtein,[48] G. Ginther,[68] T. Golling,[22] B. Gómez,[8] K. Gounder,[49] A. Goussiou,[54] P. D. Grannis,[69] S. Greder,[3] H. Greenlee,[49] Z. D. Greenwood,[58] E. M. Gregores,[4] Ph. Gris,[13] J.-F. Grivaz,[16] L. Groer,[67] S. Grünendahl,[49] M. W. Grünewald,[30] S. N. Gurzhiev,[38] G. Gutierrez,[49] P. Gutierrez,[72] A. Haas,[67] N. J. Hadley,[59] S. Hagopian,[48] I. Hall,[72] R. E. Hall,[46] C. Han,[62] L. Han,[7] K. Hanagaki,[49] K. Harder,[57] R. Harrington,[61] J. M. Hauptman,[55] R. Hauser,[63] J. Hays,[52] T. Hebbeker,[21] D. Hedin,[51] J. M. Heinmiller,[50] A. P. Heinson,[47] U. Heintz,[60] C. Hensel,[56] G. Hesketh,[61] M. D. Hildreth,[54] R. Hirosky,[77] J. D. Hobbs,[69] B. Hoeneisen,[12] M. Hohlfeld,[24] S. J. Hong,[31] R. Hooper,[73] P. Houben,[33] Y. Hu,[69] J. Huang,[53] I. Iashvili,[47] R. Illingworth,[49] A. S. Ito,[49] S. Jabeen,[56] M. Jaffré,[16] S. Jain,[72] V. Jain,[70] K. Jakobs,[23] A. Jenkins,[42] R. Jesik,[42] K. Johns,[44] M. Johnson,[49] A. Jonckheere,[49] P. Jonsson,[42] A. Juste,[49] D. Käfer,[21] W. Kahl,[57] S. Kahn,[70] E. Kajfasz,[15] A. M. Kalinin,[35] J. Kalk,[63] D. Karmanov,[37] J. Kasper,[60] D. Kau,[48] R. Kaur,[27] R. Kehoe,[75] S. Kermiche,[15] S. Kesisoglou,[73] A. Khanov,[68] A. Kharchilava,[54] Y. M. Kharzheev,[35] H. Kim,[74] B. Klima,[49] M. Klute,[22] J. M. Kohli,[27] M. Kopal,[72] V. M. Korablev,[38] J. Kotcher,[70] B. Kothari,[67] A. Koubarovsky,[37] A. V. Kozelov,[38] J. Kozminski,[63] A. Kryemadhi,[77] S. Krzywdzinski,[49] S. Kuleshov,[36] Y. Kulik,[49] A. Kumar,[28] S. Kunori,[59] A. Kupco,[11] T. Kurča,[20] J. Kvita,[11] S. Lager,[40] N. Lahrichi,[18] G. Landsberg,[73] J. Lazoflores,[48] A.-C. Le Bihan,[19] P. Lebrun,[20] W. M. Lee,[48] A. Leflat,[37] F. Lehner,[49,*] C. Leonidopoulos,[67] J. Leveque,[44] P. Lewis,[42] J. Li,[74] Q. Z. Li,[49] J. G. R. Lima,[51] D. Lincoln,[49] S. L. Linn,[48] J. Linnemann,[63] V. V. Lipaev,[38] R. Lipton,[49] L. Lobo,[42] A. Lobodenko,[39] M. Lokajicek,[11] A. Lounis,[19] P. Love,[41] H. J. Lubatti,[78] L. Lueking,[49] M. Lynker,[54] A. L. Lyon,[49] A. K. A. Maciel,[51] R. J. Madaras,[45] P. Mättig,[26] C. Magass,[21] A. Magerkurth,[62] A.-M. Magnan,[14] N. Makovec,[16] P. K. Mal,[29] H. B. Malbouisson,[3] S. Malik,[58] V. L. Malyshev,[35] H. S. Mao,[6] Y. Maravin,[49] M. Martens,[49] S. E. K. Mattingly,[73] A. A. Mayorov,[38] R. McCarthy,[69] R. McCroskey,[44] D. Meder,[24] H. L. Melanson,[49] A. Melnitchouk,[64] A. Mendes,[15] M. Merkin,[37] K. W. Merritt,[49] A. Meyer,[21] M. Michaut,[18] H. Miettinen,[76] J. Mitrevski,[67] N. Mokhov,[49] J. Molina,[3] N. K. Mondal,[29] R. W. Moore,[5] G. S. Muanza,[20] M. Mulders,[49] Y. D. Mutaf,[69] E. Nagy,[15] M. Narain,[60] N. A. Naumann,[34] H. A. Neal,[62] J. P. Negret,[8] S. Nelson,[48] P. Neustroev,[39] C. Noeding,[23] A. Nomerotski,[49] S. F. Novaes,[4] T. Nunnemann,[25] E. Nurse,[43] V. O'Dell,[49] D. C. O'Neil,[5] V. Oguri,[3] N. Oliveira,[3] N. Oshima,[49] G. J. Otero y Garzón,[50] P. Padley,[76] N. Parashar,[58] S. K. Park,[31] J. Parsons,[67] R. Partridge,[73] N. Parua,[69] A. Patwa,[70] P. M. Perea,[47] E. Perez,[18] P. Pétroff,[16] M. Petteni,[42] L. Phaf,[33] R. Piegaia,[1] M.-A. Pleier,[68] P. L. M. Podesta-Lerma,[32] V. M. Podstavkov,[49]

Y. Pogorelov,[54] B. G. Pope,[63] W. L. Prado da Silva,[3] H. B. Prosper,[48] S. Protopopescu,[70] J. Qian,[62] A. Quadt,[22] B. Quinn,[64] K. J. Rani,[29] K. Ranjan,[28] P. A. Rapidis,[49] P. N. Ratoff,[41] N. W. Reay,[57] S. Reucroft,[61] M. Rijssenbeek,[69] I. Ripp-Baudot,[19] F. Rizatdinova,[57] R. F. Rodrigues,[3] C. Royon,[18] P. Rubinov,[49] R. Ruchti,[54] V. I. Rud,[37] G. Sajot,[14] A. Sánchez-Hernández,[32] M. P. Sanders,[59] A. Santoro,[3] G. Savage,[49] L. Sawyer,[58] T. Scanlon,[42] D. Schaile,[25] R. D. Schamberger,[69] H. Schellman,[52] P. Schieferdecker,[25] C. Schmitt,[26] A. Schwartzman,[66] R. Schwienhorst,[63] S. Sengupta,[48] H. Severini,[72] E. Shabalina,[50] M. Shamim,[57] V. Shary,[18] A. A. Shchukin,[38] W. D. Shephard,[54] R. K. Shivpuri,[28] D. Shpakov,[61] R. A. Sidwell,[57] V. Simak,[10] V. Sirotenko,[49] P. Skubic,[72] P. Slattery,[68] R. P. Smith,[49] K. Smolek,[10] G. R. Snow,[65] J. Snow,[71] S. Snyder,[70] S. Söldner-Rembold,[43] X. Song,[51] L. Sonnenschein,[17] A. Sopczak,[41] M. Sosebee,[74] K. Soustruznik,[9] M. Souza,[2] B. Spurlock,[74] N. R. Stanton,[57] J. Stark,[14] J. Steele,[58] K. Stevenson,[53] V. Stolin,[36] A. Stone,[50] D. A. Stoyanova,[38] J. Strandberg,[40] M. A. Strang,[74] M. Strauss,[72] R. Ströhmer,[25] D. Strom,[52] M. Strovink,[45] L. Stutte,[49] S. Sumowidagdo,[48] A. Sznajder,[3] M. Talby,[15] P. Tamburello,[44] W. Taylor,[5] P. Telford,[43] J. Temple,[44] E. Thomas,[15] B. Thooris,[18] M. Tomoto,[49] T. Toole,[59] J. Torborg,[54] S. Towers,[69] T. Trefzger,[24] S. Trincaz-Duvoid,[17] B. Tuchming,[18] C. Tully,[66] A. S. Turcot,[70] P. M. Tuts,[67] L. Uvarov,[39] S. Uvarov,[39] S. Uzunyan,[51] B. Vachon,[5] R. Van Kooten,[53] W. M. van Leeuwen,[33] N. Varelas,[50] E. W. Varnes,[44] A. Vartapetian,[74] I. A. Vasilyev,[38] M. Vaupel,[26] P. Verdier,[16] L. S. Vertogradov,[35] M. Verzocchi,[59] F. Villeneuve-Seguier,[42] J.-R. Vlimant,[17] E. Von Toerne,[57] M. Vreeswijk,[33] T. Vu Anh,[16] H. D. Wahl,[48] R. Walker,[42] L. Wang,[59] Z.-M. Wang,[69] J. Warchol,[54] G. Watts,[78] M. Wayne,[54] M. Weber,[49] H. Weerts,[63] M. Wegner,[21] N. Wermes,[22] A. White,[74] V. White,[49] D. Wicke,[49] D. A. Wijngaarden,[34] G. W. Wilson,[56] S. J. Wimpenny,[47] J. Wittlin,[60] M. Wobisch,[49] J. Womersley,[49] D. R. Wood,[61] T. R. Wyatt,[43] Q. Xu,[62] N. Xuan,[54] S. Yacoob,[52] R. Yamada,[49] M. Yan,[59] T. Yasuda,[49] Y. A. Yatsunenko,[35] Y. Yen,[26] K. Yip,[70] H. D. Yoo,[73] S. W. Youn,[52] J. Yu,[74] A. Yurkewicz,[69] A. Zabi,[16] A. Zatserklyaniy,[51] M. Zdrazil,[69] C. Zeitnitz,[24] D. Zhang,[49] X. Zhang,[72] T. Zhao,[78] Z. Zhao,[62] B. Zhou,[62] J. Zhu,[69] M. Zielinski,[68] D. Zieminska,[53] A. Zieminski,[53] R. Zitoun,[69] V. Zutshi,[51] and E. G. Zverev[37]

(D0 Collaboration)

[1]*Universidad de Buenos Aires, Buenos Aires, Argentina*
[2]*LAFEX, Centro Brasileiro de Pesquisas Físicas, Rio de Janeiro, Brazil*
[3]*Universidade do Estado do Rio de Janeiro, Rio de Janeiro, Brazil*
[4]*Instituto de Física Teórica, Universidade Estadual Paulista, São Paulo, Brazil*
[5]*University of Alberta, Edmonton, Alberta, Canada, Simon Fraser University, Burnaby, British Columbia, Canada, York University, Toronto, Ontario, Canada, and McGill University, Montreal, Quebec, Canada*
[6]*Institute of High Energy Physics, Beijing, People's Republic of China*
[7]*University of Science and Technology of China, Hefei, People's Republic of China*
[8]*Universidad de los Andes, Bogotá, Colombia*
[9]*Center for Particle Physics, Charles University, Prague, Czech Republic*
[10]*Czech Technical University, Prague, Czech Republic*
[11]*Institute of Physics, Academy of Sciences, Center for Particle Physics, Prague, Czech Republic*
[12]*Universidad San Francisco de Quito, Quito, Ecuador*
[13]*Laboratoire de Physique Corpusculaire, IN2P3-CNRS, Université Blaise Pascal, Clermont-Ferrand, France*
[14]*Laboratoire de Physique Subatomique et de Cosmologie, IN2P3-CNRS, Universite de Grenoble 1, Grenoble, France*
[15]*CPPM, IN2P3-CNRS, Université de la Méditerranée, Marseille, France*
[16]*Laboratoire de l'Accélérateur Linéaire, IN2P3-CNRS, Orsay, France*
[17]*LPNHE, IN2P3-CNRS, Universités Paris VI and VII, Paris, France*
[18]*DAPNIA/Service de Physique des Particules, CEA, Saclay, France*
[19]*IReS, IN2P3-CNRS, Université Louis Pasteur, Strasbourg, France, and Université de Haute Alsace, Mulhouse, France*
[20]*Institut de Physique Nucléaire de Lyon, IN2P3-CNRS, Université Claude Bernard, Villeurbanne, France*
[21]*III. Physikalisches Institut A, RWTH Aachen, Aachen, Germany*
[22]*Physikalisches Institut, Universität Bonn, Bonn, Germany*
[23]*Physikalisches Institut, Universität Freiburg, Freiburg, Germany*
[24]*Institut für Physik, Universität Mainz, Mainz, Germany*
[25]*Ludwig-Maximilians-Universität München, München, Germany*
[26]*Fachbereich Physik, University of Wuppertal, Wuppertal, Germany*
[27]*Panjab University, Chandigarh, India*
[28]*Delhi University, Delhi, India*
[29]*Tata Institute of Fundamental Research, Mumbai, India*
[30]*University College Dublin, Dublin, Ireland*
[31]*Korea Detector Laboratory, Korea University, Seoul, Korea*

[32]CINVESTAV, Mexico City, Mexico
[33]FOM-Institute NIKHEF and University of Amsterdam/NIKHEF, Amsterdam, The Netherlands
[34]Radboud University Nijmegen/NIKHEF, Nijmegen, The Netherlands
[35]Joint Institute for Nuclear Research, Dubna, Russia
[36]Institute for Theoretical and Experimental Physics, Moscow, Russia
[37]Moscow State University, Moscow, Russia
[38]Institute for High Energy Physics, Protvino, Russia
[39]Petersburg Nuclear Physics Institute, St. Petersburg, Russia
[40]Lund University, Lund, Sweden, Royal Institute of Technology and Stockholm University, Stockholm, Sweden, and Uppsala University, Uppsala, Sweden
[41]Lancaster University, Lancaster, United Kingdom
[42]Imperial College, London, United Kingdom
[43]University of Manchester, Manchester, United Kingdom
[44]University of Arizona, Tucson, Arizona 85721, USA
[45]Lawrence Berkeley National Laboratory and University of California, Berkeley, California 94720, USA
[46]California State University, Fresno, California 93740, USA
[47]University of California, Riverside, California 92521, USA
[48]Florida State University, Tallahassee, Florida 32306, USA
[49]Fermi National Accelerator Laboratory, Batavia, Illinois 60510, USA
[50]University of Illinois at Chicago, Chicago, Illinois 60607, USA
[51]Northern Illinois University, DeKalb, Illinois 60115, USA
[52]Northwestern University, Evanston, Illinois 60208, USA
[53]Indiana University, Bloomington, Indiana 47405, USA
[54]University of Notre Dame, Notre Dame, Indiana 46556, USA
[55]Iowa State University, Ames, Iowa 50011, USA
[56]University of Kansas, Lawrence, Kansas 66045, USA
[57]Kansas State University, Manhattan, Kansas 66506, USA
[58]Louisiana Tech University, Ruston, Louisiana 71272, USA
[59]University of Maryland, College Park, Maryland 20742, USA
[60]Boston University, Boston, Massachusetts 02215, USA
[61]Northeastern University, Boston, Massachusetts 02115, USA
[62]University of Michigan, Ann Arbor, Michigan 48109, USA
[63]Michigan State University, East Lansing, Michigan 48824, USA
[64]University of Mississippi, University, Mississippi 38677, USA
[65]University of Nebraska, Lincoln, Nebraska 68588, USA
[66]Princeton University, Princeton, New Jersey 08544, USA
[67]Columbia University, New York, New York 10027, USA
[68]University of Rochester, Rochester, New York 14627, USA
[69]State University of New York, Stony Brook, New York 11794, USA
[70]Brookhaven National Laboratory, Upton, New York 11973, USA
[71]Langston University, Langston, Oklahoma 73050, USA
[72]University of Oklahoma, Norman, Oklahoma 73019, USA
[73]Brown University, Providence, Rhode Island 02912, USA
[74]University of Texas, Arlington, Texas 76019, USA
[75]Southern Methodist University, Dallas, Texas 75275, USA
[76]Rice University, Houston, Texas 77005, USA
[77]University of Virginia, Charlottesville, Virginia 22901, USA
[78]University of Washington, Seattle, Washington 98195, USA

(Received 18 February 2005; published 27 July 2005)

We present a measurement of the $Z\gamma$ production cross section and limits on anomalous $ZZ\gamma$ and $Z\gamma\gamma$ couplings for form-factor scales of $\Lambda = 750$ and 1000 GeV. The measurement is based on 138 (152) candidates in the $ee\gamma$ ($\mu\mu\gamma$) final state using 320(290) pb^{-1} of $p\bar{p}$ collisions at $\sqrt{s} = 1.96$ TeV. The 95% C.L. limits on real and imaginary parts of individual anomalous couplings are $|h^Z_{10,30}| < 0.23$, $|h^Z_{20,40}| < 0.020$, $|h^\gamma_{10,30}| < 0.23$, and $|h^\gamma_{20,40}| < 0.019$ for $\Lambda = 1000$ GeV.

DOI: 10.1103/PhysRevLett.95.051802 PACS numbers: 12.15.Ji, 13.38.Dg, 13.40.Em, 13.85.Qk

Studies of events containing pairs of vector bosons provide important tests of the standard model (SM) of electroweak interactions. In the SM, the trilinear gauge couplings of the Z boson to the photon are zero; therefore,

photons do not interact with Z bosons at lowest order. Evidence for such an interaction would indicate new physics [1].

We present a new study of $Z\gamma$ production in $p\bar{p}$ collisions using Z boson decays to e^+e^- and $\mu^+\mu^-$, where the dilepton system can be produced by either an on-shell Z boson, or a virtual Z boson or γ (the Drell-Yan process). The dilepton plus photon final state, $\ell^+\ell^-\gamma$, can be produced in the SM through either of two processes. The photon may be emitted through initial state radiation (ISR) from one of the partons in the p or $\bar{p}$, or produced as final state radiation (FSR) from one of the final state leptons. We collectively refer to these processes as $Z\gamma$ production.

The SM $Z\gamma$ processes produce photons with a rapidly falling transverse energy, E_T^γ. In contrast, anomalous $ZZ\gamma$ and $Z\gamma\gamma$ couplings, which appear in extensions of the SM, can cause production of photons with high E_T^γ and can increase the $\ell^+\ell^-\gamma$ cross section compared to the SM prediction. Below we describe a search for this anomalous production within the framework of Ref. [2]. This formalism assumes only that the $ZV\gamma$ ($V = Z, \gamma$) couplings are Lorentz and gauge invariant. The most general $ZV\gamma$ coupling is parametrized by two CP-violating (h_1^V and h_2^V) and two CP-conserving (h_3^V and h_4^V) complex coupling parameters. Partial wave unitarity is ensured at high energies by using a form-factor ansatz $h_i^V = h_{i0}^V/(1 + \hat{s}/\Lambda^2)^{n_i}$ ($i = 1, \ldots, 4$), where $\sqrt{\hat{s}}$ is the parton center-of-mass energy, Λ is the form-factor scale, and n_i is the form-factor power. We set the form-factor powers $n_1 = n_3 = 3$ and $n_2 = n_4 = 4$, in accordance with Ref. [2].

Previous studies of Z boson and photon production have been made by the CDF [3] and D0 [4] Collaborations using $p\bar{p}$ collisions, and by the DELPHI [5], L3 [6], and OPAL [7] Collaborations using e^+e^- collisions. The combined LEP results are available in Ref. [8].

The data for this analysis were collected by the D0 Run II detector at the Fermilab Tevatron Collider with $p\bar{p}$ center-of-mass energy $\sqrt{s} = 1.96$ TeV between April 2002 and June 2004. The integrated luminosities used for this analysis are 320 pb^{-1} for the electron final state and 290 pb^{-1} for the muon final state.

The D0 detector [9] consists of an inner tracker, surrounded by liquid-argon/uranium calorimeters, and a muon spectrometer. The detector subsystems provide measurements over the full range of azimuthal angle ϕ [10] and over different, overlapping regions of detector pseudorapidity η. The inner tracker consists of a silicon microstrip tracker (SMT) and a central fiber tracker (CFT), both located within a 2 T superconducting solenoidal magnet. The CFT and the SMT have coverage out to $|\eta| \lesssim 1.8$ and $|\eta| \lesssim 3.0$, respectively. The calorimeter is divided into a central calorimeter (CC) covering the range $|\eta| < 1.1$ and two end calorimeters (EC) housed in separate cryostats, which extend coverage to $|\eta| \approx 4$. The calorimeters are longitudinally segmented into electromagnetic (EM) and hadronic sections. The muon system lies outside the calorimeters and consists of tracking detectors, scintillation trigger counters, and a 1.8 T toroid magnet. It has coverage up to $|\eta| \approx 2.0$. Luminosity is measured using plastic scintillator arrays located in front of the EC cryostats, covering $2.7 < |\eta| < 4.4$.

The data were collected with a three-level trigger system (L1, L2, and L3). We require that the events in the electron decay channel satisfy one of the high-E_T single electron triggers, while the events in the muon decay channel must fire one of the high-p_T single or dimuon triggers. At L1 the single electron triggers select events based on the energy deposited in the EM section of the calorimeter; typical L1 requirements are greater than 10–15 GeV. At L3, additional requirements are imposed on the fraction of energy deposited in the EM calorimeter and the shape of the energy deposition. The efficiency of the electron trigger requirement is about 80% for an electron with $E_T \approx 25$ GeV and more than 98% for $E_T > 30$ GeV. The muon trigger requires hits in the muon system scintillators at L1, and in portions of the data set also requires spatially matched hits in the muon tracking detectors. At L2, muon track segments are reconstructed and p_T requirements are imposed. At L3, some of the triggers used in this analysis require events to have a track reconstructed in the inner tracker with p_T greater than 10 GeV. The logical OR of single and dimuon triggers has an efficiency of 92% for muons from Z boson decay.

Electrons are reconstructed as clusters of energy in the calorimeter. These clusters are required to have 90% of their energy deposited in the EM calorimeter (in either the central calorimeter $|\eta| < 1.1$ or the end calorimeter $1.5 < |\eta| < 2.5$). We require that the longitudinal and transverse shower shape of the cluster is consistent with that expected from an electron and that the cluster is isolated from other activity in the calorimeter. Electron candidates in the central calorimeter are required to have spatially matched tracks. At least one electron candidate must be identified in the CC region, and at least one is required to have $p_T > 25$ GeV/c. Muons are identified by a central track matched to segments in the muon system. The muon must be within $|\eta| < 2.0$. To reduce potential contamination from muons produced in b-quark decays of $b\bar{b}$ events, we impose isolation requirements on the muon candidates in both the calorimeter and the central tracker. To remove the background from cosmic ray muons, muon tracks must originate from the beam region and more than 0.05 radians from exactly back to back.

Z boson candidates are reconstructed by requiring a pair of high-p_T ($p_T > 15$ GeV/c) electrons or muons that form an invariant mass above 30 GeV/c^2.

In addition to a Z boson candidate, we require events to have a photon candidate, with a separation from both leptons of $\Delta\mathcal{R} = \sqrt{(\phi_\ell - \phi_\gamma)^2 + (\eta_\ell - \eta_\gamma)^2} > 0.7$ and

with $E_T^\gamma > 8$ GeV. Photons are reconstructed as energy clusters in the central calorimeter. The transverse shower shape of the cluster must be consistent with that expected from a photon. We also require a photon candidate to deposit at least 90% of its energy in the EM calorimeter and to be isolated from other activity in the calorimeter and the tracker.

Muon and electron detection efficiencies for the above requirements are determined using a sample of $Z \to \ell\ell$ candidates. In the electron channel the combined trigger and reconstruction efficiency is measured to be $(73 \pm 4)\%$. In the muon channel it is measured to be $(81 \pm 4)\%$. The photon identification efficiency is measured as a function of E_T^γ using a Monte Carlo simulation. A systematic uncertainty of 4% is assessed from the difference between the simulated electrons and electron candidates in $Z \to ee$ data, and the difference between simulated electrons and photons. The photon identification efficiency is E_T-dependent and rises from about 75% at 8 GeV to about 90% above 27 GeV.

Background from processes with photons and leptons from misidentified jets is found to be negligible. Contributions from $Z(\to \tau^+\tau^-)\gamma$ production with leptonic decays of the tau are less than 1% of the sample and thus neglected. The only significant source of background to $Z\gamma$ production is from Z + jets processes in which a jet is misidentified as a photon. We estimate the Z + jets background by folding the jet-E_T spectrum in Z + jets candidates with the probability for a jet to be misidentified as a photon. The probability is measured as a function of the photon candidate's E_T using a sample of events dominated by QCD multijet processes. The misidentification probability is about 5×10^{-3} and decreases with E_T. We correct the misidentification probability for direct photon production (γ + jets) by fitting the photon candidate E_T distribution to the functional form derived in [11]. For low E_T ($E_T < 75$ GeV) this contribution is measured to be 9% of the probability, and we take this number as a systematic uncertainty.

We use an event generator employing leading order (LO) QCD calculations and first order electroweak radiation with a detector simulation tuned with Z boson candidates to calculate the acceptances for the data and expected rates from both the SM and anomalous $Z\gamma$ production [2]. We use the CTEQ6L [12] parton distribution function (PDF) set. We estimate the uncertainty due to the PDF choice to be 3.3% using the prescription in Ref. [13]. Using a next to leading order (NLO) $Z\gamma$ Monte Carlo [14] generator, we calculate an E_T^γ-dependent K factor to parametrize the effect of E_T^γ-dependent NLO corrections in the LO Monte Carlo sample. The value of the K factor is approximately 1.15 for $E_T^\gamma = 10$ GeV, and increases to $\approx$ 1.3 for $E_T^\gamma = 100$ GeV. The uncertainty due to the choice of K factor (flat with a value of 1.34 vs E_T^γ dependent) is found to be negligible.

We observe 138 events in the electron channel, to be compared to the SM estimate of 95.3 ± 4.9 $e^+e^-\gamma$ events and 23.6 ± 2.3 background events. In the muon channel, we observe 152 events while SM estimates are 126.0 ± 7.8 events and 22.4 ± 3.0 background events. The uncertainty in the SM signal is dominated by the uncertainty in the lepton and photon reconstruction efficiencies, and that in the background estimation is dominated by the uncertainty in the jet misidentification probability.

The E_T spectrum for photon candidates is shown in Fig. 1 with the estimation of the total SM prediction and its QCD background component overlaid. The highest transverse energy photon in the electron channel is 105 GeV, while the highest transverse energy photon in the muon channel is 166 GeV. In Fig. 2 we plot the three-body mass ($M_{\ell\ell\gamma}$) against the dilepton mass ($M_{\ell\ell}$) for each event in the data. The dilepton and three-body mass distributions are given in Fig. 3. The ISR events with a dilepton system produced by an on-shell Z boson populate a vertical band at $M_{\ell\ell}$ around Z boson mass, M_Z, and $M_{\ell\ell\gamma} > M_Z$. The on-shell Z boson FSR events cluster along a horizontal band at $M_{\ell\ell\gamma} = M_Z$ and have $M_{\ell\ell} < M_Z$. The Drell-Yan events populate the diagonal band with $M_{\ell\ell} \approx M_{\ell\ell\gamma}$ extending from the lower left to the upper right corner of the plot.

For events satisfying the phase space requirements, $\Delta\mathcal{R}_{\ell\gamma} > 0.7$, $E_T^\gamma > 8$ GeV, and $M_{\ell\ell} > 30$ GeV$/c^2$, the combined cross section times branching ratio is measured to be $4.2 \pm 0.4(\text{stat} + \text{syst}) \pm 0.3(\text{lumin})$ pb, where the first uncertainty includes contributions from statistics and

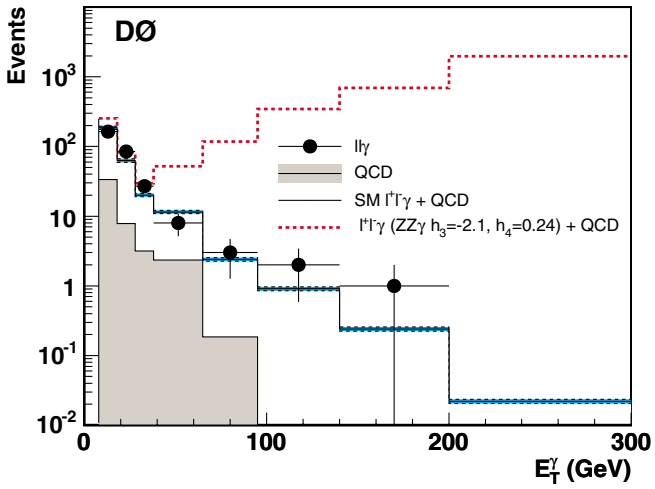

FIG. 1 (color online). Photon candidate E_T spectrum for $\ell\ell\gamma$ data (solid circles), QCD multijet background (shaded histogram), the Monte Carlo simulation of the $\ell^+\ell^-\gamma$ production with anomalous $ZZ\gamma$ ($h_3 = -2.1$, $h_4 = 0.24$) coupling (dashed histogram), and the standard model plus background (solid histogram). The shaded band is the systematic uncertainty on the SM plus background. The Monte Carlo distribution is normalized to the luminosity.

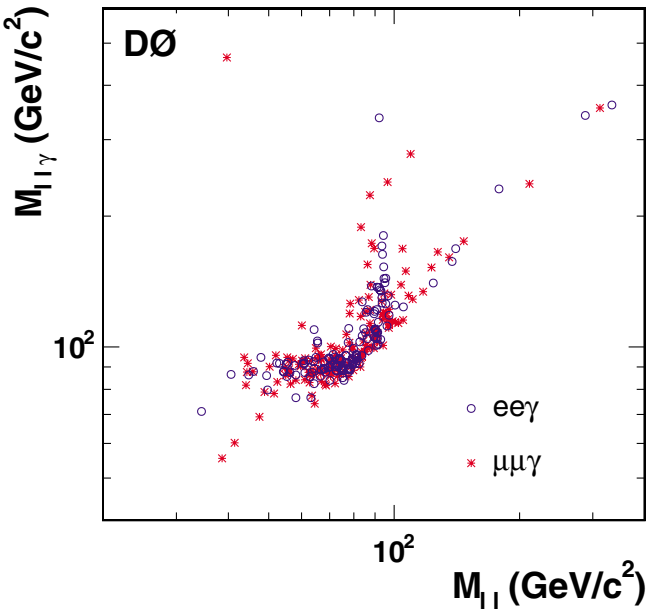

FIG. 2 (color online). Dilepton + photon vs dilepton mass of $Z\gamma$ candidates. Candidates in the electron channel are shown as empty circles, while the muon mode candidates are shown as stars.

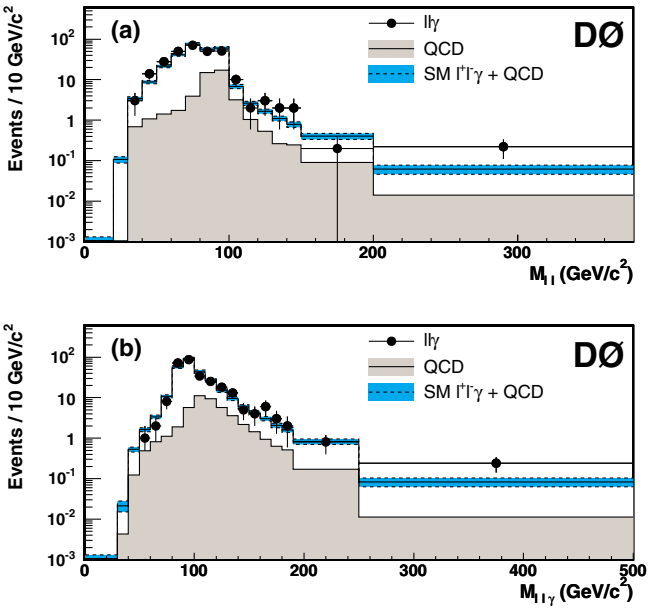

FIG. 3 (color online). (a) Dilepton mass and (b) dilepton + photon mass of $\ell\ell\gamma$ data (solid circles), QCD multijet background (shaded histogram), and the standard model plus background (histogram). The shaded band is the systematic uncertainty on the SM plus background. The Monte Carlo distribution is normalized to the luminosity.

all systematic effects except the luminosity, and the second is due to the luminosity measurement uncertainty [15]. This value is in agreement with the expected value of $3.9\,^{+0.1}_{-0.2}$ pb from NLO theory calculations [14]. The largest systematic uncertainty is due to photon identification, while lepton identification, PDF uncertainty, and background model are of similar magnitude.

Given the separation exhibited in Fig. 2, we can measure a cross section of ISR-enhanced $Z\gamma$ production. By minimizing the effects of final state radiation, one is able to examine the contribution from initial state radiation in more detail. With the additional requirements that the dilepton mass and three-body mass exceed 65 and 100 GeV$/c^2$, respectively, the SM Monte Carlo simulation indicates that 80% of the remaining events are due to initial state radiation. For this restricted sample we observe 55 and 62 events in the electron and muon channels, respectively. The expectation for signal events is 31.1 and 37.9, while background expectations are 18.6 and 14.7 events in the electron and muon channels, respectively. The cross section times branching ratio is measured to be $1.07 \pm 0.15(\text{stat + syst}) \pm 0.07(\text{lumin})$ pb, in agreement with the expected $0.94\,^{+0.02}_{-0.05}$ pb [14].

Given the good agreement observed between the data and the SM prediction, we extract upper limits on anomalous couplings [16]. We generate Monte Carlo events in a two-dimensional grid of CP-violating anomalous couplings (h^V_{10} and h^V_{20}) and do the same for CP-conserving (h^V_{30} and h^V_{40}) anomalous couplings. We calculate the likelihood of the agreement between the E^γ_T distribution of the 290 data events (shown in Fig. 1) to the estimated background and Monte Carlo simulation for each point of the grid. Assuming Poisson statistics for the data and Gaussian systematic uncertainties, we extract the 95% C.L. limits on each of the anomalous couplings while assuming the others are zero. The limits on CP-violating and CP-conserving anomalous couplings are nearly identical. We also find the limits on real and imaginary parts of the couplings to be similar as well. We present the limits on both real and imaginary parts of the CP-conserving and CP-violating couplings in Table I. The two-dimensional limit contours on individual CP-conserving couplings are shown in Fig. 4.

TABLE I. Summary of the 95% C.L. upper limits on the anomalous couplings. Limits are set by allowing only the real or imaginary part of one coupling to vary; all others are fixed to their standard model values. As indicated, we find upper limits on CP-conserving and CP-violating parameters to be nearly identical. We also find that nearly identical limits apply to the real or imaginary parts of all couplings.

Coupling	$\Lambda = 750$ GeV	$\Lambda = 1$ TeV
$\lvert\text{Re}(h^Z_{10,30})\rvert$, $\lvert\text{Im}(h^Z_{10,30})\rvert$	0.24	0.23
$\lvert\text{Re}(h^Z_{20,40})\rvert$, $\lvert\text{Im}(h^Z_{20,40})\rvert$	0.027	0.020
$\lvert\text{Re}(h^\gamma_{10,30})\rvert$, $\lvert\text{Im}(h^\gamma_{10,30})\rvert$	0.29	0.23
$\lvert\text{Re}(h^\gamma_{20,40})\rvert$, $\lvert\text{Im}(h^\gamma_{20,40})\rvert$	0.030	0.019

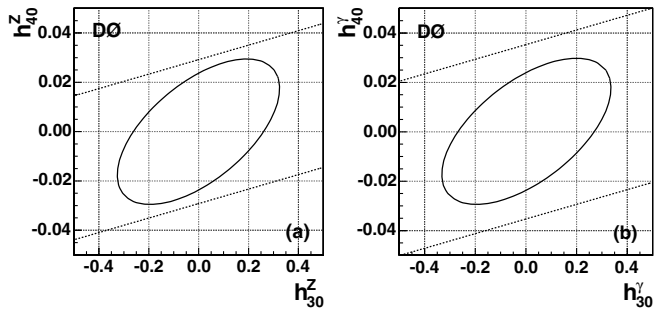

FIG. 4. The 95% C.L. two-dimensional exclusion limits for *CP*-conserving (a) $ZZ\gamma$ and (b) $Z\gamma\gamma$ couplings for $\Lambda = 1$ TeV. Dashed lines illustrate the unitarity constraints.

In conclusion, we have studied a sample of 290 $\ell\ell\gamma$ events, consistent with $Z\gamma$ production. This sample exceeds that previously collected by D0 by an order of magnitude. This is due to 3 times more integrated luminosity, an increased production cross section associated with the 10% higher center-of-mass energy, and significant improvements in particle detection efficiency achieved with the D0 Run II upgrade. The $\ell\ell\gamma$ cross section is measured to be $4.2 \pm 0.4(\text{stat} + \text{syst}) \pm 0.3(\text{lumin})$ pb. After additional selection requirements, most of the final state radiation is removed, leaving the sample dominated by initial state radiation. The cross section for this ISR-enhanced $Z\gamma$ production is measured to be $1.07 \pm 0.15(\text{stat} + \text{syst}) \pm 0.07(\text{lumin})$ pb. These values are consistent with the SM expectations. We observe no significant deviation from the SM expectation in the total cross section or photon E_T distribution, and thus extract limits on anomalous $Z\gamma$ couplings. The one-dimensional limits at 95% C.L. for both *CP*-conserving and *CP*-violating couplings (both real and imaginary parts) are $|h^Z_{10,30}| < 0.23$, $|h^Z_{20,40}| < 0.020$, $|h^\gamma_{10,30}| < 0.23$, and $|h^\gamma_{20,40}| < 0.019$ for $\Lambda = 1$ TeV. These limits are substantially more restrictive than previous results that have been presented using this formalism [4]. Accounting for the different formalism used at LEP, our limits on h^V_{20} and h^V_{40} are more than twice as restrictive as the combined results of the four LEP experiments [17].

We thank the staffs at Fermilab and collaborating institutions, and acknowledge support from the Department of Energy and National Science Foundation (USA), Commissariat á l'Energie Atomique and CNRS/Institut National de Physique Nucléaire et de Physique des Particules (France), Ministry of Education and Science, Agency for Atomic Energy, and RF President Grants Program (Russia), CAPES, CNPq, FAPERJ, FAPESP, and FUNDUNESP (Brazil), Departments of Atomic Energy and Science and Technology (India), Colciencias (Colombia), CONACyT (Mexico), KRF (Korea), CONICET and UBACyT (Argentina), The Foundation for Fundamental Research on Matter (The Netherlands), PPARC (United Kingdom), Ministry of Education (Czech Republic), Canada Research Chairs Program, CFI, Natural Sciences and Engineering Research Council, and WestGrid Project (Canada), BMBF and DFG (Germany), Science Foundation Ireland, A. P. Sloan Foundation, Research Corporation, Texas Advanced Research Program, Alexander von Humboldt Foundation, and the Marie Curie Program.

*Visitor from University of Zurich, Zurich, Switzerland.

[1] G. J. Gounaris, J. Layssac, and F. M. Renard, Phys. Rev. D **67**, 013012 (2003); **61**, 073013 (2000).
[2] U. Baur and E. L. Berger, Phys. Rev. D **47**, 4889 (1993).
[3] D. Acosta *et al.* (CDF Collaboration), Phys. Rev. Lett. **94**, 041803 (2005); F. Abe *et al.* (CDF Collaboration), Phys. Rev. Lett. **74**, 1941 (1995).
[4] B. Abbott *et al.* (D0 Collaboration), Phys. Rev. D **57**, R3817 (1998); S. Abachi *et al.* (D0 Collaboration), Phys. Rev. Lett. **78**, 3640 (1997); S. Abachi *et al.* (D0 Collaboration), Phys. Rev. Lett. **75**, 1028 (1995).
[5] P. Abreu *et al.* (DELPHI Collaboration), Phys. Lett. B **380**, 480 (1996).
[6] M. Acciarri *et al.* (L3 Collaboration), Phys. Lett. B **436**, 187 (1998); P. Achard *et al.* (L3 Collaboration), Phys. Lett. B **597**, 119 (2004).
[7] G. Abbiendi *et al.*, Eur. Phys. J. C **17**, 553 (2000).
[8] D. Abbaneo *et al.* (LEP Collaborations), hep-ex/0412015.
[9] V. Abazov *et al.*, Nucl. Instrum. Methods Phys. Res., Sect. A (to be published); T. LeCompte and H. T. Diehl, Annu. Rev. Nucl. Part. Sci. **50**, 71 (2000).
[10] We use a cylindrical coordinate system about the beam pipe in which positive z is along the proton direction, θ is the polar angle, ϕ is the azimuthal angle, and pseudorapidity (η) is defined as $-\ln(\tan(\theta/2))$.
[11] S. Abachi *et al.* (D0 Collaboration), Phys. Rev. Lett. **77**, 5011 (1996).
[12] J. Pumplin *et al.* (CTEQ Collaboration), J. High Energy Phys. 07 (2002) 012.
[13] D. Stump *et al.* (CTEQ Collaboration), J. High Energy Phys. 10 (2003) 046.
[14] U. Baur, T. Han, and J. Ohnemus, Phys. Rev. D **57**, 2823 (1998).
[15] T. Edwards *et al.*, Report No. FERMILAB-TM-2278-E, 2004.
[16] We set limits on anomalous couplings using the 290 $Z\gamma$ candidates that satisfied the following phase space requirements: $\Delta\mathcal{R}_{\ell\gamma} > 0.7$, $E^\gamma_T > 8$ GeV, and $M_{\ell\ell} > 30$ GeV$/c^2$.
[17] S. Eidelman *et al.*, Phys. Lett. B **592**, 1 (2004); LEP electroweak working group, http://www.cern.ch/LEPEWWG/lepww/tgc.